Large area flat crystal x-ray spectrometer with high integrated intensity for an electron beam ion trap

Nobuyuki Nakamura[a)]
Cold Trapped Ions Project, ICORP, JST, 1-40-2 Fuda, Chofu, Tokyo 182-0024, Japan

(Received 27 June 2000; accepted for publication 29 August 2000)

A flat crystal x-ray spectrometer has been constructed for spectroscopic studies of highly charged ions with an electron beam ion trap. It consists of a flat crystal and a position sensitive proportional counter. Employment of a flat crystal yields easy alignment, easy processing of the crystal, and high flexibility. The proportional counter has been designed to have a large effective area, which is needed to compensate for weak focusing power of a flat crystal. The utility of the new spectrometer has been demonstrated with the Tokyo electron beam ion trap. © *2000 American Institute of Physics.* [S0034-6748(90)01212-6]

I. INTRODUCTION

An electron beam ion trap (EBIT)[1,2] is a versatile device to study highly charged ions. It was designed especially for spectroscopic studies, where many remarkable studies[3,4] have been carried out. Since x-ray radiation is dominant for transitions in highly charged ions, most spectroscopic studies have been devoted to the x-ray region. In those studies, spectrometers of the von Hámos type,[5] the Johann type,[6] the DuMond type,[7] and the flat type[8–10] have been used. Since a flat crystal spectrometer has no focusing power in the nondispersive direction and only intrinsic focusing power in the dispersive direction, its throughput is generally low compared to the curved crystal spectrometers. However, a flat crystal spectrometer is frequently used for studies with an EBIT because it has several merits as below.

First, processing of a crystal is easier; no bending process is needed at all. This provides such advantages that not only is the price of the crystal comparatively cheap but also the quality of the crystal is not disturbed by the bending process. Second, alignment is much easier because there is no focusing mechanism. Since the x-ray radiation from an EBIT is relatively weak, it is practically difficult to align a spectrometer by observing the radiation. It is also difficult to put a laser, an x-ray tube, or other intense sources at the center of the ion trap, i.e., the actual source position. Therefore, it usually takes many hours to align curved crystal spectrometers so that the best performance is obtained. On the other hand, simple geometrical arrangement always gives good alignment for a flat crystal spectrometer. Third, the dimensions, i.e., the optical path length, is independent of the objective wavelength. Furthermore, it is not very important to make the distance between the source and the crystal and the distance between the crystal and the detector the same. These characteristics make the adjustment of a flat crystal spectrometer flexible. While for curved crystal spectrometers, when the radius of curvature of a crystal is fixed, the dimensions are uniquely determined from the objective wavelength. It means that the resolution and the luminosity depend on the objective wavelength.

This article describes a new flat crystal spectrometer with high efficiency and flexibility constructed for spectroscopic studies with the Tokyo EBIT.[1] A large area proportional counter is used to compensate for the lack of focusing power in the nondispersive direction, which sets the present spectrometer apart from other flat crystal spectrometers used in the spectroscopic studies with EBITs. Consequently, high effective luminosity has been achieved which is comparable to curved crystal spectrometers such as a von Hámos, and a Johann spectrometer. Merits and demerits of the present spectrometer are discussed through demonstration with the Tokyo EBIT.

II. DESIGN

A. Spectrometer

Figure 1 shows a schematic diagram of the present spectrometer. A detailed description of the Tokyo EBIT has been given in previous articles.[11,12,1] In the EBIT, the electron beam is compressed by a strong magnetic field to a diameter of about 60 μm and excites the trapped ions. On the other hand, the source height is limited to 10 mm by the observation window in the ion trap. Consequently, the source in the EBIT is a line source, and thus it requires no entrance slit. Accordingly, spectrometers of the flat type as well as the von Hámos type are well suited to spectroscopic studies with an EBIT.

The spectrometer is operated in vacuo to avoid x-ray attenuation. The spectrometer mainly consists of two vacuum chambers, one of which is for the crystal and another for the detector. A bellows nipple (bellows *B*) which can change the angle of the detector port by $\pm 15°$ and an adapter nipple which has an angle of 30° between the two flanges are used for angle adjustment. A combination of them allows us to operate the spectrometer for the Bragg angle range 22.5°–67.5°. For the Bragg angle range 37.5°–52.5°, the adapter is not used, and only the bellows nipple is used for angle adjustment [Fig. 1(a)]. For the Bragg angle

a)Electronic mail: nakamura@hci.jst.go.jp

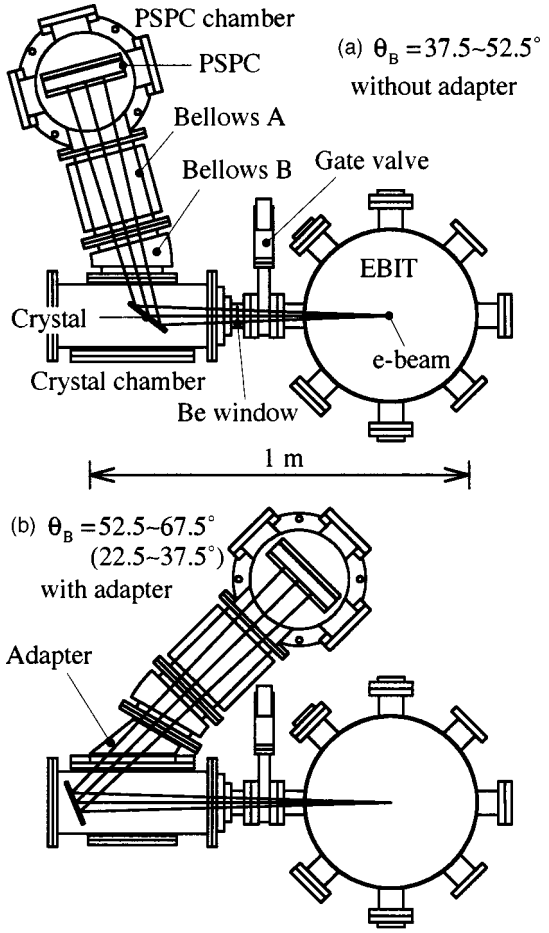

FIG. 1. Schematic layout of the new flat crystal spectrometer. (a) Arrangement for the Bragg angle range 37.5°–52.5°. The bellows *B* is attached to the crystal chamber directly and used for angle adjustment. (b) Arrangement for the Bragg angle range 52.5°–67.5°. An adapter nipple is attached between the bellows *B* and the crystal chamber. For the Bragg angle range 22.5°–37.5°, the adapter is overturned and attached between the bellows *B* and the crystal chamber.

range 22.5°–37.5° or 52.5°–67.5°, the adapter is attached between the crystal chamber and the bellows nipple [Fig. 1(b)]. The crystal can be moved by about 350 mm along the incident axis on the table in the crystal chamber to fit to the exit axis with different Bragg angles as shown in the figure. The distance between the source and the crystal can be changed by adding vacuum nipples between the EBIT and the crystal chamber. The distance between the crystal and the detector can also be changed in a similar way or by adjusting the length of the bellows nipple *A*. The vacuum of the spectrometer ($\sim 10^{-6}$ Torr) is separated from that of the EBIT ($\sim 10^{-9}$ Torr) with a 50 μm thick Be window. To prevent the window from braking, a bypass with a valve is installed as an additional vacuum line though it is not shown in the figure. The valve is opened when the gate valve between the EBIT and the spectrometer is closed (i.e., during preparation), and closed when the gate valve is opened (i.e., during operation).

The detectable x-ray energy range of the present spectrometer is shown in Fig. 2 for Si(111), LiF(200), and SiO_2(203) crystals. Although the detectable range can be shifted by using other crystals with a lattice constant of different values or by using higher order reflection, the efficiency of the detector may limit the range for practical use of the spectrometer as described in Sec. II B. The nominal resolving power of the spectrometer is given by

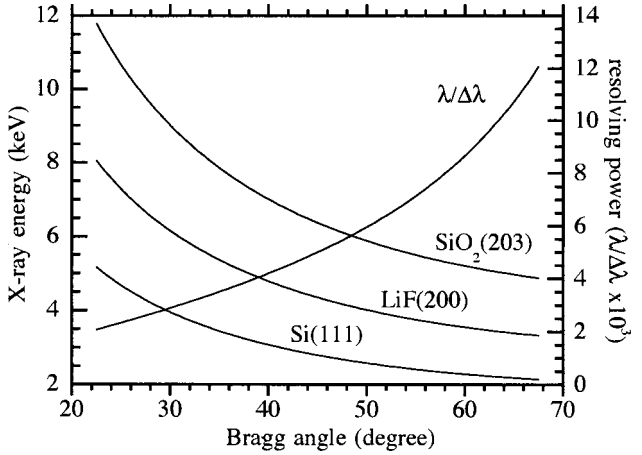

FIG. 2. Detectable x-ray energy range of the present spectrometer. Only the first order of reflection is considered. The resolving power $\lambda/\Delta\lambda$ [see Eq. (1)] is also shown for $\Delta x = 300$ μm and $D = 1500$ mm.

$$\frac{\lambda}{\Delta\lambda} = \tan\theta \cdot \frac{D}{\Delta x}, \tag{1}$$

where θ is the Bragg angle, D the distance from the source and the detector, and Δx the change in position on the detector. In the present case, the main contribution to Δx is spacial resolution of the detector. The nominal resolving power calculated for $D = 1500$ mm and $\Delta x = 300$ μm is also plotted in Fig. 2.

B. Two dimensional position sensitive proportional counter (PSPC)

As described in Sec. I, a flat crystal spectrometer has only a weak focusing character. One of the ways to compensate for it is to use a detector with a large effective area.[13] In principle, by using a detector whose effective height is twice the height of the crystal, the actual detection efficiency of a flat crystal spectrometer becomes the same as a von Hámos spectrometer. However, employment of a detector with a large effective height may give rise to one problem. Since the image of the x rays diffracted from a flat crystal is part of an arc, simple integration of the image along the direction of x-ray dispersion makes the spectral resolution worse, which appears in the case where a one-dimensional detector is used. This effect becomes more conspicuous by the large effective height. We then need to use a two-dimensional position sensitive detector and to correct the curved image.

Figure 3 shows a schematic diagram of the present PSPC newly constructed and the data acquisition system. The PSPC consists of a Be entrance window, anode wires, and a cathode of the backgammon type. The area of the Be window is 100×103 mm^2, which is in contrast to 100×30 mm^2 for the previous PSPC.[14] Actually, since there are ten horizontal ribs 1.5 mm thick to support the Be window, the effective area is 100×88 mm^2. The Be sheet of 0.8 mm thick can stand a pressure difference of five atmospheres. The win-

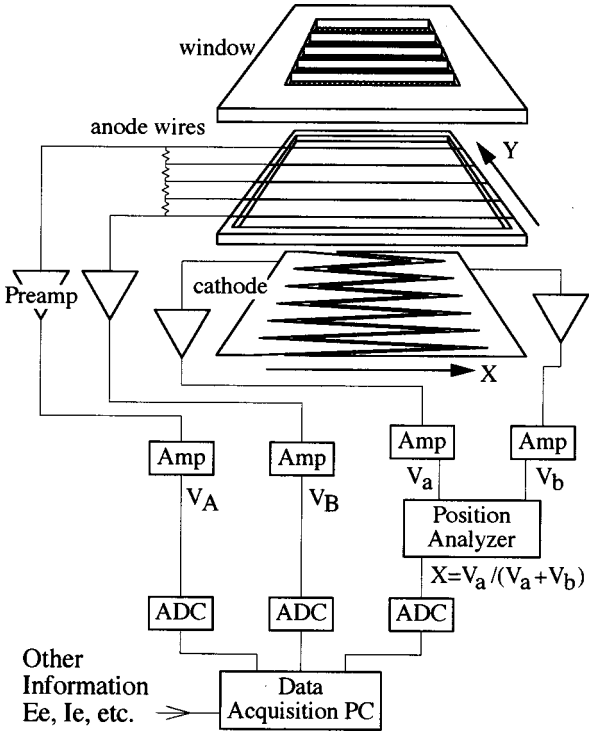

FIG. 3. Schematic diagram of the new PSPC and electronics. The anode wire and the backgammon cathode are put in a stainless box which is not shown in the figure. The box is covered with the window and filled with detection gas at 5 atm at the maximum. For the *X* direction, an analog position analyzer is used for the charge division, while the *Y* position is calculated by the data acquisition computer. The data acquisition system is capable of four input, so that other information, e.g., electron energy (*Ee*) or current (*Ie*), can be recorded at the same time.

dow holder is made of a stainless steel plate of 13 mm thick. The design of the window part is similar to that in the PSPC constructed by Vogel *et al.*[15] The anode wires are Au plated W wires with a diameter of 5 μm. At intervals of 5 mm, 23 wires have been soldered with tension of about 1.5 g. All wires are connected in series with resistors of 2 kΩ (so the total resistance is 44 kΩ) for vertical position readout (denoted *Y* direction), and both ends are connected to pre- and main amplifiers. The *Y* position is thus determined by the charge division technique.[16] The position readout in the *Y* direction is made at the intervals of the wires, i.e., 5 mm, which is enough for the correction of the curved image. Similarly to the previous one, the present PSPC employs a cathode of the backgammon type[17] for horizontal position readout (denoted *X* direction). The backgammon pattern was etched on a printed circuit board of 1.6 mm thick. The wedges with a length of 120 mm was etched at intervals of 1.6 mm. The number of the wedges is about 80, so the backgammon pattern has an area of about 120×130 mm^2.

The distance between the window and the wire is 2 mm, and that between the wire and the cathode is 2 mm. The effective thickness of the detector is thus 4 mm, which was determined so that spacial resolution should not be disturbed by the oblique incidence of the diffracted x rays. The efficiency of the detector, which is calculated from the transmittance at the Be window and the absorption by the detection gas, is shown in Fig. 4. In this calculation, we used the

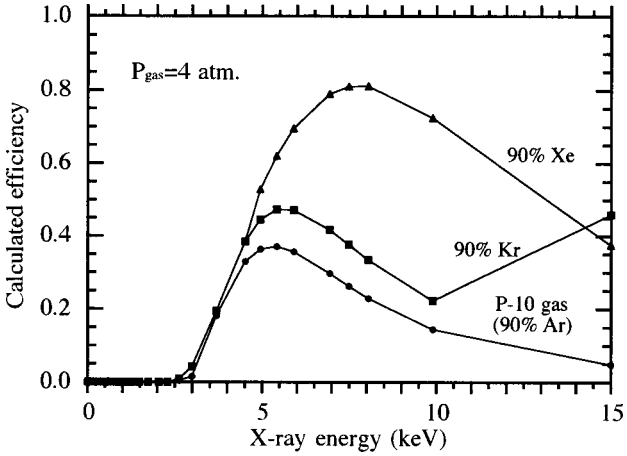

FIG. 4. Calculated efficiency of the new PSPC. The pressure of the fill gas is assumed to be 4 atm with 10% quenching gas (i.e., the pressure of ''detection'' gas is assumed to be 3.6 atm). Although the maximum pressure is designed to be 5 atm, typical operational pressure is 4 atm for the safety of the Be window.

theoretical absorption coefficients calculated by Henke *et al.*[18] Also, the quenching gas such as CH_4 may contribute the efficiency, which was not taken into account in the calculation. For a P-10 gas (Ar+10% CH_4), which is most frequency used, the detectable range is 3.5–10 keV. When the angle of x-ray incidence is normal to the face of the detector, the efficiency can be increased by increasing the effective thickness.

The spacial resolution of the PSPC was measured with a collimated x-ray beam. An aperture with a diameter of 50 μm was placed at 120 mm away from an x-ray tube whose focal size is about 0.3 mm in diameter. The PSPC was then placed at 30 mm away from the aperture. This arrangement should give an x-ray beam with a diameter of about 150 μm incident on the PSPC. The diameter of the beam was actually measured to be 140 μm at the face of the PSPC. Figure 5 shows images of the collimated x-ray beam. Three images were taken by moving the x-ray beam by using a stepping motor controlled translation stage. The width of the image

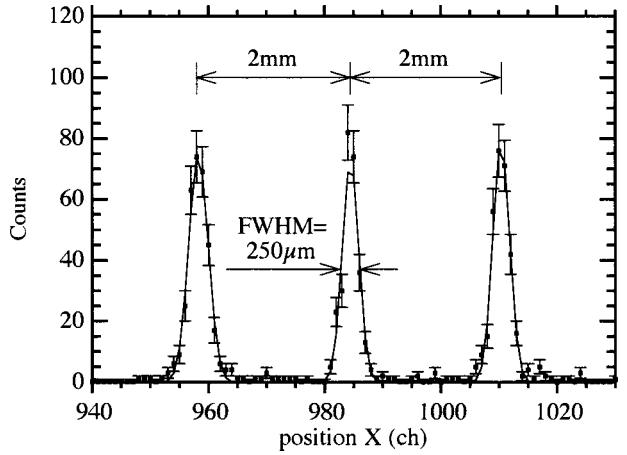

FIG. 5. Images of a collimated x-ray beam taken to determine the position resolution of the new PSPC. A solid line represents the fitted Gaussian profiles. By taking the x-ray beam width into account, position resolution of 200 μm is deduced from the image width.

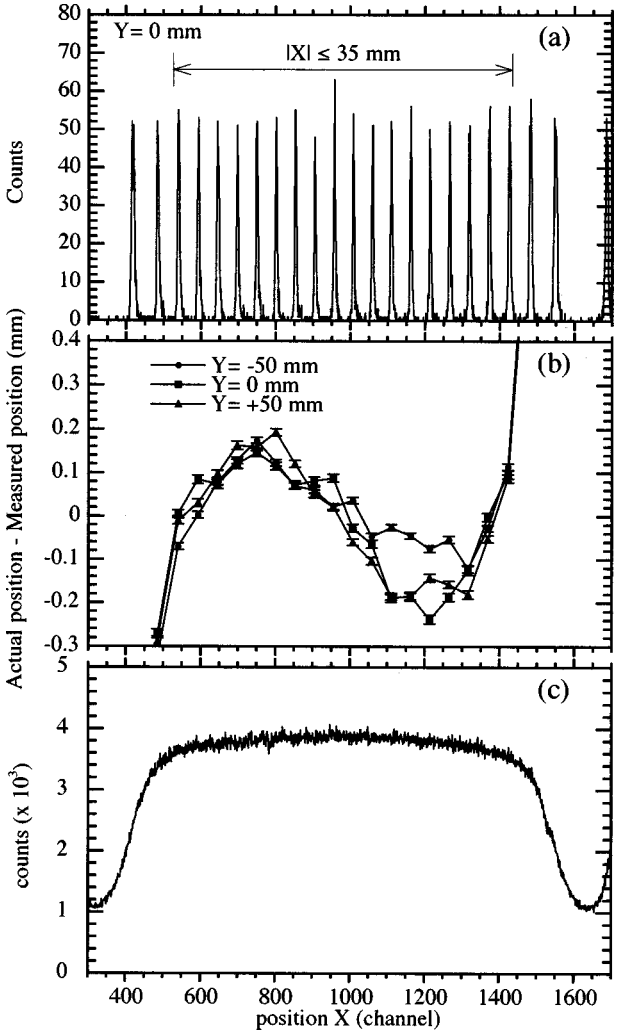

FIG. 6. (a) Images of a collimated x-ray beam taken to measure the integral linearity of the position readout. The intervals between the peaks were adjusted to be 4 mm by using a linear motion stage controlled with a stepping motor. (b) Integral nonlinearity, i.e., variation between measured and actual positions. Data for $Y=-50$ mm and $Y=+50$ mm are also shown. (c) Image of uniform illumination taken to measure the differential linearity.

was determined to be 250 μm [full width at half maximum (FWHM)]. By taking the size of the beam into account, the position resolution was estimated to be 200 μm (FWHM). However, when the PSPC is installed in the spectrometer, it is difficult to have the best performance because of the long wiring and the large electric noise in the laboratory. The ''actual'' position resolution is considered to be about 300 μm typically when the PSPC is operated in the spectrometer.

The linearity of position readout is also an important character for the detector. The integral linearity was measured in the same way as the position resolution measurement. Figure 6(a) shows the x-ray images taken by moving the beam at intervals of 4 mm. The integral nonlinearity, i.e., variation between measured and actual positions, is plotted in Fig. 6(b). In the region of $|X|\leqslant 35$ mm, the deviations are within ± 200 μm, which corresponds to integral nonlinearity of 0.3%. Since the deviations are not larger than the position resolution and better linearity can be obtained locally, the present integral nonlinearity is acceptable in most of wavelength measurements.

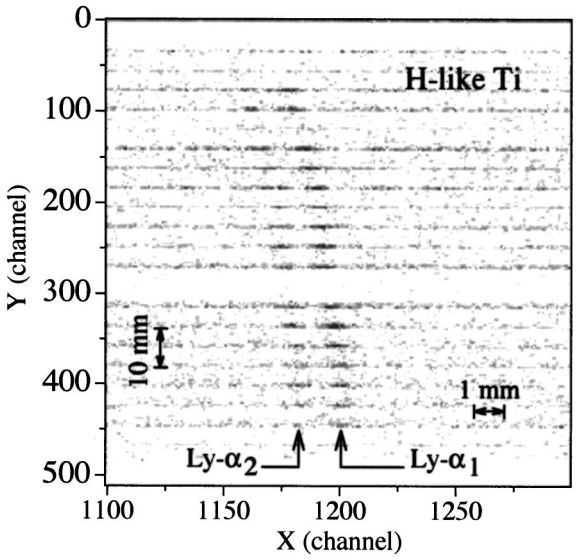

FIG. 7. Two-dimensional image on the PSPC in observation of Ly-α_1 and α_2 in hydrogenlike Ti^{21+}. Disappearance of signals at $Y\sim 290$ channel is owing to lack of the corresponding wire at that time.

The differential nonlinearity was measured by illuminating the PSPC with the x-ray tube (without a collimating aperture) which was placed at about 1 m away from the PSPC. This arrangement gave uniform illumination on the PSPC. As shown in Fig. 6(c), the differential nonlinearity is within $\pm 5\%$ for the region of $|X|\leqslant 35$ mm. Considering that better linearity can be obtained locally, the present differential nonlinearity is acceptable in most intensity measurements. It is concluded from the present results that the useful range of the present PSPC is $|X|\leqslant 35$ mm when the linearity of position readout is important.

III. PERFORMANCE

In order to see the total characteristics of the spectrometer, spectroscopic observations were performed for x-ray radiations from different species of highly charged ions pro-

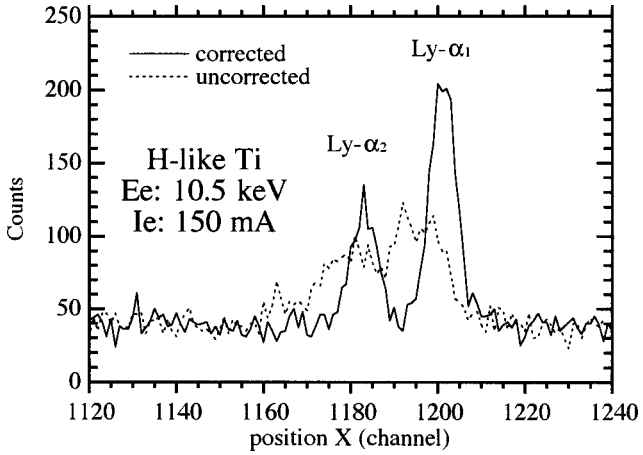

FIG. 8. Spectrum of Ly-α_1 and α_2 in hydrogenlike Ti^{21+} obtained by integrating the image shown in Fig. 7. A dotted line represents the spectrum obtained by integrating the image without correction. A solid line represents the corrected spectrum obtained by integrating the image after correcting the curved image. *Ee* and *Ie* represent the electron energy and the current at which the spectrum was obtained.

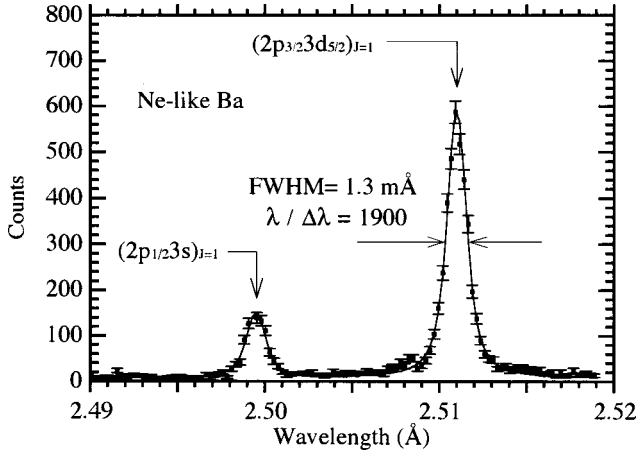

FIG. 9. Spectrum for $n=3-2$ transitions in neonlike Ba^{46+}. A solid line represents the fitted Voigt line shapes.

duced in the Tokyo EBIT. Lyman-α_1 $(2p_{3/2}\rightarrow 1s)$ and Lyman-α_2 $(2p_{1/2}\rightarrow 1s)$ in hydrogen-like Ti^{21+} were observed with a Si(111) crystal. The first order of reflection was used, so that the Bragg angle was 23°. The distance between the source (electron beam) and the crystal was 770 mm and the distance between the crystal and the PSPC was 700 mm. The P-10 gas was used for the present PSPC. Figure 7 shows a two-dimensional image obtained on the PSPC. It took 30 h to obtain this spectrum with a 10.5 keV–150 mA electron beam. As shown in the figure, the spectral lines are not straight. If an one-dimensional detector had been used, these lines would be integrated along the vertical direction. The integrated spectrum is shown in Fig. 8 by a dotted line. A solid line represents the corrected spectrum obtained after correcting the curved image. The present observation clearly demonstrates the advantage for the two-dimensional detection.

Figure 9 shows the spectrum for $n=3-2$ transitions in neonlike Ba^{46+} obtained with a LiF(200) crystal. The first order of reflection was also used, so that the Bragg angle was 38°. The distance between the source (electron beam) and the crystal was 650 mm and the distance between the crystal and the PSPC was 340 mm. The P-10 gas was also used. It took 7 h to obtain this spectrum with a 7.7 keV–110 mA electron beam. A solid line in the figure represents Voigt line shapes fitted to the data. The spectral line width is 1.3 mÅ (FWHM) which corresponds to $\lambda/\Delta\lambda=1900$. The nominal resolving power for this arrangement is about 2500 by assuming the spacial resolution of the PSPC to be 0.3 mm. The difference between the actual and the nominal resolving power is considered to arise from the fact that the angular width of a reflection curve has a finite value. In the measurement for the rocking curve of the LiF(200) crystal used in the present observation, it was found that the measured curve has a Lorentzian-like shape. Therefore, the fact that the spectral line shape in Fig. 9 is a Voigt profile rather than a Gaussian profile supports the above consideration. It is noted that the natural and the Doppler width are much smaller than the present spectral width.[19]

In summary, we have constructed a flexible flat crystal x-ray spectrometer with high detection efficiency for spectroscopic studies with the Tokyo electron beam ion trap. For this spectrometer, a two-dimensional position sensitive proportional counter (PSPC) was also constructed as a detector. The PSPC was designed to have a large effective area to compensate for the weak focusing power of a flat crystal. The characteristics of this detector, such as position resolution and the linearity of position readout, have been confirmed to be satisfactory for the new spectrometer. The utility of the new spectrometer has been demonstrated through observations of hydrogenlike Ti and neonlike Ba produced with the Tokyo EBIT.

ACKNOWLEDGMENTS

The author is grateful to Dr. Mizogawa and Dr. Isozumi for giving us useful information in the course of the design. The author also appreciates fruitful discussion with the YEBISU group, including N. Miura who helped to construct the PSPC.

[1] N. Nakamura *et al.*, Rev. Sci. Instrum. **69**, 694 (1998).
[2] R. E. Marrs, M. A. Levine, D. A. Knapp, and J. R. Henderson, Phys. Rev. Lett. **60**, 1715 (1988).
[3] P. Beiersdorfer, S. R. Elliott, J. C. López-Urrutia, and K. Widmann, Nucl. Phys. A **626**, 357c (1997).
[4] K. Widmann, P. Beiersdorfer, J. R. C. López-Urrutia, and S. Elliott, Hyperfine Interact. **108**, 73 (1997).
[5] P. Beiersdorfer, R. E. Marrs, J. R. Henderson, D. A. Knapp, M. A. Levine, D. B. Platt, M. B. Schneider, D. A. Vogel, and K. L. Wong, Rev. Sci. Instrum. **61**, 2338 (1990).
[6] T. E. Cowan, C. L. Bennett, D. D. Dietrich, J. V. Bixler, C. J. Hailey, J. R. Henderson, D. A. Knapp, M. A. Levin, R. E. Marrs, and M. B. Schneider, Phys. Rev. Lett. **66**, 1150 (1991).
[7] K. Widmann, P. Beiersdorfer, G. V. Brown, J. R. C. López-Urrutia, V. Decaux, and D. W. Savin, Rev. Sci. Instrum. **68**, 1087 (1997).
[8] P. Beiersdorfer and B. J. Wargelin, Rev. Sci. Instrum. **65**, 13 (1994).
[9] G. V. Brown, P. Beiersdorfer, and K. Widmann, Rev. Sci. Instrum. **70**, 280 (1999).
[10] D. Klöpfel, Hölzer, E. Förster, and P. Beiersdorfer, Rev. Sci. Instrum. **68**, 3669 (1997).
[11] F. J. Currell *et al.*, J. Phys. Soc. Jpn. **65**, 3186 (1996).
[12] H. Watanabe *et al.*, J. Phys. Soc. Jpn. **66**, 3795 (1997).
[13] T. Mizogawa, Phys. Scr., T **T73**, 403 (1997).
[14] N. Nakamura, D. Kato, E. Nojikawa, F. J. Currell, A. Y. Faenov, T. A. Pikuz, and S. Ohtani, Phys. Scr., **T80**, 443 (1999).
[15] D. Vogel, P. Beiersdorfer, V. Decaux, and K. Widmann, Rev. Sci. Instrum. **66**, 776 (1995).
[16] G. W. Fraser, *X-ray Detectors in Astronomy* (Cambridge University Press, Cambridge, 1989).
[17] T. Mizogawa, Y. Awaya, Y. Isozumi, R. Katano, S. Ito, and N. Maeda, Nucl. Instrum. Methods Phys. Res. A **312**, 547 (1992).
[18] B. L. Henke, E. M. Gullikson, and J. C. Davis, At. Data Nucl. Data Tables **54**, 181 (1993).
[19] P. Beiersdorfer, A. L. Osterheld, V. Decaux, and K. Widmann, Phys. Rev. Lett. **77**, 5353 (1996).